The structure of plasma dissociated zircon

Evans, Williamson and Glasser [1] have recently suggested that the structure of plasma dissociated zircon (PDZ) is influenced by metastable liquid–liquid immiscibility in the ZrO_2–SiO_2 system because of undercooling of molten droplets during their passage through the plasma furnace. The present authors have reached somewhat similar conclusions [2] but suggest a different microstructural interpretation which is briefly outlined in this note.

A sample of PDZ, prepared at the National Physical Laboratory, Teddington, UK, using a 100 kW plasma reactor [3], was studied. It consisted of spheroidized particles with diameters predominantly within the range 125 to 250 μm and was reported to be 99% dissociated. X-ray diffraction showed that the sample consisted mainly of the monoclinic form of ZrO_2, although some tetragonal ZrO_2 was also detected. Silica was not detected either as a crystalline or amorphous phase, presumably because the high X-ray absorption of Zr effectively shields the underlying material reducing the intensity of the amorphous, diffuse peak; the strong line of the only likely crystalline phase of SiO_2, cristobalite, would have been apparent, if present.

Optical transmission microscopy of thin sections of the PDZ revealed a radial growth pattern of bi-refringent material in some particles with a structure too fine to be resolved, but most particles appeared homogeneous with no apparent structure. Scanning electron microscopy (SEM), using a back-scattered electron detector to provide atomic number contrast, showed, within the resolution limits of the detector, an apparently featureless structure in most particles. Some particles, however, had a surface cellular substructure similar to that previously reported by Charles *et al.* [4] and Evans and Williamson [5]. The detailed structure within the cells varied from particle to particle ranging from a fine spherulitic pattern of ZrO_2 in SiO_2 (Fig. 1a) to rather more regular crystals of ZrO_2 radiating from a central, circular region (Fig. 1b and c).

Transmission electron microscopy (TEM) was carried out on thin chips of the PDZ prepared by crushing. The predominant structure revealed in this way was of small particles of monoclinic ZrO_2 in an SiO_2 glass matrix (Fig. 2). This appearance could have arisen either from a distribution of isolated equiaxed particles or from cross-sections

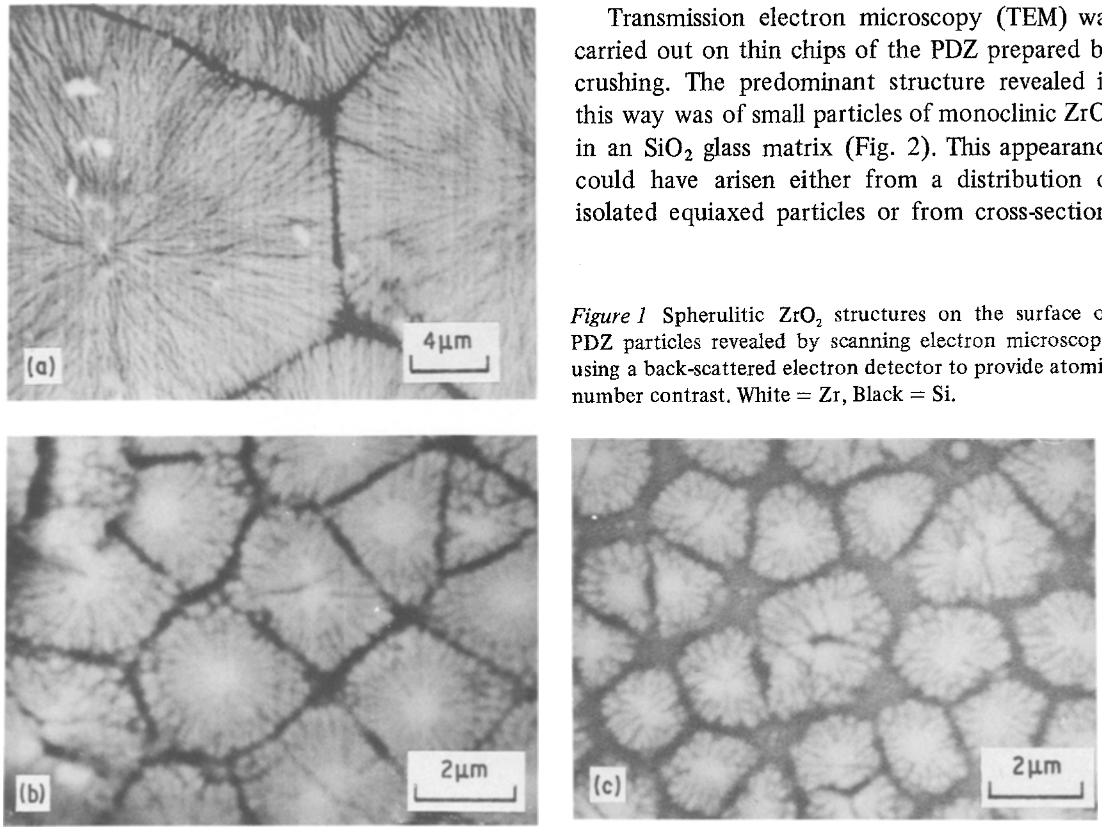

Figure 1 Spherulitic ZrO_2 structures on the surface of PDZ particles revealed by scanning electron microscopy using a back-scattered electron detector to provide atomic number contrast. White = Zr, Black = Si.

0022–2461/81/061732–04$02.40/0

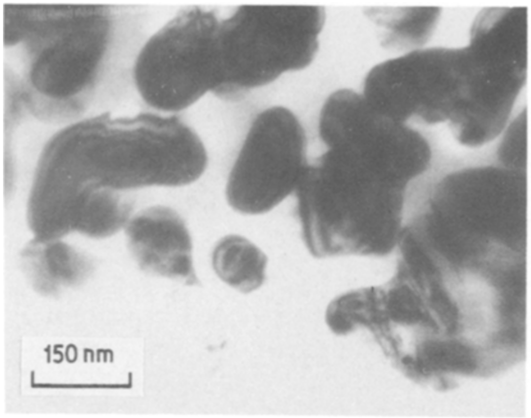

Figure 2 Transmission electron micrograph of PDZ fragment showing monoclinic ZrO_2 crystals dispersed in SiO_2-rich glass.

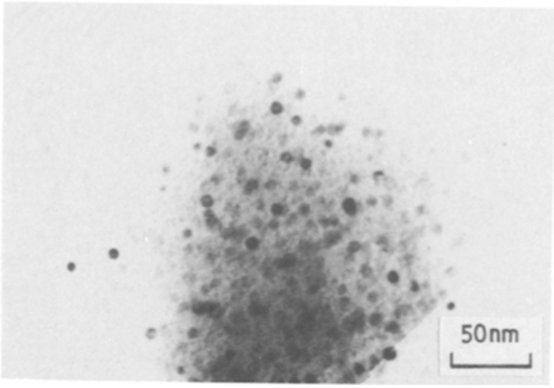

Figure 3 Transmission electron micrograph of PDZ fragment showing spherical tetragonal ZrO_2 crystals dispersed in SiO_2-rich glass.

of fibrous crystals. Some regions showing a finer distribution of spherical crystals of ZrO_2 in glass were also observed and these were found to have the tetragonal structure (Fig. 3). To obtain a better indication of the morphology of the ZrO_2, a sample of PDZ was treated with 10% hydrofluoric acid, to dissolve the SiO_2 matrix, and a suspension of the resulting particles was dispersed on a carbon film for TEM. The microstructures observed consisted of branched crystals with a range of cross-sectional diameters (Fig. 4), together with some spherical particles with diameters which were in the range from approximately 5 to 50 nm.

As previously discussed in detail [6], completely molten plasma spheroidized particles generally undercool to approximately $0.8\,T_m$, where T_m is the equilibrium melting point (in K) before crystallisation is nucleated because they are isolated from each other and do not contain pre-existing nuclei. The microstructure finally observed depends upon the relative nucleation kinetics of alternative phases, the rates of transformation of one phase to another and the thermal history of the particle during and after solidification. The latter in turn depends upon crystal growth rate, the particle diameter and the surface heat transfer coefficient.

The generally accepted ZrO_2–SiO_2 phase diagram shows a miscibility gap with a consolute point at approximately 55 wt % SiO_2 and 2430° C [7]. The data on which this diagram is based is sparse in the high-temperature region and the extent of the miscibility gap is not known with any great accuracy. Theoretical considerations have led Galakhov and Varshal [8] to suggest that the metastable miscibility gap is rather wide and extends from 0–80 wt % ZrO_2 at 1080° C. This, and the liquidus data of Toropov and Galakhov [9], have been used to construct the ZrO_2 liquidus and metastable miscibility gap in the vicinity of the zircon composition, as shown in Fig. 5. The estimated nucleation temperature of ZrO_2 from the liquid is also shown, based on a maximum under-cooling of 20% of the absolute liquidus temperature.

The very low interfacial energy between liquid phases [10] would be expected to considerably reduce the undercooling required for homogeneous nucleation of liquid–liquid phase separation compared with crystallisation. The close proximity of the metastable miscibility gap co-existence line to the estimated nucleation curve for ZrO_2 for zircon composition liquid (Fig. 5) therefore suggests that either homogeneous nucleation of ZrO_2 crystals or phase separation into ZrO_2 and SiO_2 liquids may be possible during the cooling of isolated droplets. Phase separation would result in the formation of a ZrO_2-rich liquid with composition such that tetragonal ZrO_2 would crystallize from it almost immediately with rejection of SiO_2 into the remaining liquid phase. The resulting microstructure would thus tend to consist of a fine dispersion of ZrO_2 in a SiO_2-rich glass.

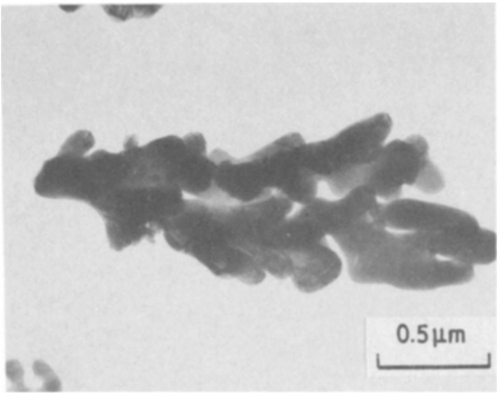

Figure 4 Transmission electron micrograph of ZrO_2 crystals separated from PDZ by treatment with dilute HF.

The present PDZ sample seems to consist predominantly of ZrO_2 crystals with a branched morphology. The cellular microstructure revealed by SEM in many of the particles is consistent with the growth of ZrO_2 nuclei in a spherulitic manner, that is, radial growth accompanied by branching of the crystal arms. The material between the ZrO_2 fibrous crystals would then be a SiO_2-rich glass, and the high SiO_2-content regions between individual spherulites (Fig. 1) would correspond to the SiO_2-rich residual liquid remaining at the outer boundary of the spherulites when crystallisation of ZrO_2 was complete.

The generally accepted explanation for spherulite formation involves instability of crystal growth because of compositional gradients in high viscosity melts [11]. The diameter of the fibrous crystals, δ, is given by

$$\delta = D/G, \tag{1}$$

where D is the relevant diffusion coefficient and G is the crystal growth rate. The different morphologies of ZrO_2 spherulites observed are thus consistent with growth at different temperatures (D and G will both be sensitive functions of temperature). The spherulitic structure could then have arisen either by growth from homogeneously nucleated ZrO_2 or from pre-existing ZrO_2 crystallites present because of incomplete melting of the particles.

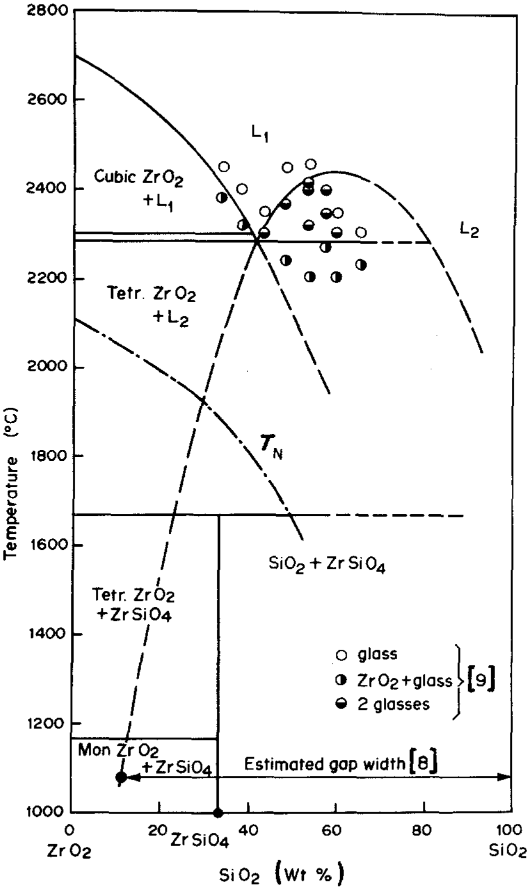

Figure 5 Part of the ZrO_2–SiO_2 phase diagram based on the data of Galakhov and Varshal [8], and Toropov and Galakhov [9]. The curve marked T_N is the estimated homogeneous nucleation temperature for ZrO_2 ($0.8\,T_m$).

It would be surprising if all particles treated in the plasma furnace were completely melted because of the range of possible thermal histories arising from their different trajectories. Particles heated above the temperature at which the viscosity was sufficiently low to allow spheroidization in the time available, but not heated to above a temperature necessary to produce a homogeneous liquid phase, would consist of tetragonal or cubic ZrO_2 dispersed in a silica-rich liquid. The ZrO_2 particles would be expected to grow during subsequent cooling at a rate determined by the diffusion rate of Zr-ions in the surrounding liquid. The spherulitic structures observed are thus consistent with growth at different temperatures, suggesting spherulite formation both from pre-existing nuclei remaining in partly-melted particles and from homogeneously nucleated ZrO_2.

The liquid in metastable equilibrium with the

ZrO_2 as it crystallized from the melt in the temperature range 1900 to 2300° C (from the extension of the liquidus) would lie within the miscibility gap and it could therefore separate into ZrO_2-rich and SiO_2-rich liquids followed by crystallization of tetragonal ZrO_2 from the ZrO_2-rich phase. The regions consisting of very fine spherical particles of tetragonal ZrO_2 in glass (Fig. 3), could have arisen in this way. The retention of the tetragonal form rather than transformation to the equilibrium monoclinic structure on cooling is consistent with particle size and matrix restraint stabilization effects [12].

In summary, the most likely explanation for the structures of the PDZ sample studied is as follows:

The majority of particles have completely melted and ZrO_2 has nucleated from the liquid phase at high undercooling to give a dispersion of ZrO_2 in SiO_2 glass. Some particles have not completely melted and the unmelted ZrO_2 crystals have acted as nuclei for subsequent crystal growth during cooling between the liquidus temperature and approximately 1900° C. ZrO_2 nuclei have grown in a spherultic manner, the detailed structure of the spherulites being a function of the undercooling at which growth occurred. The growth of ZrO_2 spherulites can result in phase separation in the remaining liquid phase with the formation of spherical ZrO_2 crystallites, some of which are small enough to persist as the metastable tetragonal form on cooling. Further work is necessary to determine whether spherulitic growth of ZrO_2 occurs in all particles and if phase separation is restricted to the material between spherulite crystals or is of general occurrence in some particles.

Acknowledgement

Thanks are due to Mr R. K. Bayliss of N.P.K., Teddington, for supplying the PDZ and to Dr R. A. Jago and Mr. K. Richter for assistance with the electron microscopy.

References

1. A. M. EVANS, J. P. H. WILLIAMSON and F. P. GLASSER, *J. Mater, Sci.* **15** (1980) 2325.
2. AI MING WONG and R. McPHERSON, Proceedings of the 9th Australian Ceramic Conference, Sydney, August 1980 (Australian Ceramic Society, University of New South Wales, Kensington, NSW, 1980) p. 213.
3. R. K. BAYLISS, J. W. BRYANT and J. G. SAYCE, Proceeding of the 3rd International Symposium on Plasma Chemistry, IUPAC/University of Limoges, France, July, 1977 (IUPAC/University of Limoges, 1977) paper S.J.2.
4. J. A. CHARLES, G. J. DAVIES, R. M. JERVIS and G. THURSFIELD, *Trans. Inst. Min. Met.* 79 (1970) 54C.
5. A. M. EVANS and J. P. H. WILLIAMSON, *J. Mater. Sci.* **12** (1977) 779.
6. R. McPHERSON, *ibid.* 8 (1973) 851.
7. W. C. BUTTERMAN and W. R. FOSTER, *Amer. Min.* 52 (1967) 884.
8. F. Ya. GALAKHOV and G. G. VARSHAL, in "The Structures of Glass" edited by E. A. Porai-Koshits. Vol. 8 (Consultants Bureau, New York, 1973) p. 7.
9. N. A. TOROPOV and F. Ya. GALAKHOV, *Bull. Acad. Sci. USSR Div. Chem. Sci.* (1956) 153.
10. J. J. HAMMEL, *J. Chem. Phys.* **46** (1967) 2234.
11. H. D. KEITH and F. J. PADDEN, *J. Appl. Phys.* **34** (1963) 2409.
12. R. C. GARVIE, *J. Phys. Chem.* **82** (1978) 218.

Received 27 October
and accepted 2 December 1980

AI MING WONG
R. McPHERSON
Department of Materials Engineering,
Monash University,
Clayton,
Victoria 3168,
Australia